

## SYNTHETIC, STRUCTURAL AND PE SPECTROSCOPIC STUDIES ON BIS(PENTADIENYL) COMPOUNDS OF IRON, RUTHENIUM AND OSMIUM. THE ROLE OF THE HEAVY METAL

LOTHAR STAHL, HUAIRANG MA, RICHARD D. ERNST\*

*Department of Chemistry, University of Utah, Salt Lake City, Utah 84112 (U.S.A.)*

ISABELLA HYLAKRYSPIK, ROLF GLEITER\*

*Organisch-Chemisches Institut der Universität Heidelberg, D-6900 Heidelberg (West Germany)*

and MANFRED L. ZIEGLER\*

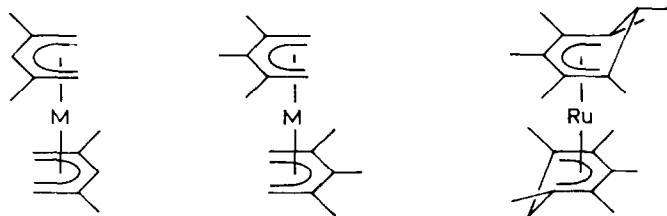
*Anorganisch-Chemisches Institut der Universität Heidelberg, D-6900 Heidelberg (West Germany)*

(Received November 19th, 1986)

### Summary

The syntheses of bis(2,3,4-trimethylpentadienyl)iron and bis(2,4-dimethylpentadienyl)osmium are reported, as well as their variable temperature NMR behaviour and a single-crystal X-ray diffraction study for the latter compound. All data indicate that these complexes adopt a *gauche*-eclipsed conformation in the ground state. Photoelectron spectra have also been obtained for these complexes, and suggest that the radical cations of bis(pentadienyl)iron complexes differ significantly from their ruthenium and osmium counterparts.

It has recently been demonstrated that replacement of a first row transition metal by a heavier congener can be used to spread out the PE bands (the “heavy metal effect”) [1]. This was first demonstrated for the bis( $\eta^3$ -allyl) compounds of nickel,



M = Fe (1)

M = Ru (2)

M = Os (3)

M = Fe (4)

M = Ru (5)

(6)

palladium, and platinum [1,2], as well as for the  $\eta^3$ -allyl(tetracarbonyl) complexes of manganese and rhenium [1,3]. In this study we present our results on the bis( $\eta^5$ -2,4-dimethylpentadienyl) complexes of iron (**1**) [4], ruthenium (**2**) [5], and osmium (**3**), as well as on the bis( $\eta^5$ -2,3,4-trimethylpentadienyl) complexes of iron (**4**) and ruthenium (**5**) [6] and bis( $\eta^5$ -1,2,3,4,5,6-hexamethylcyclohexadienyl)ruthenium (**6**) [7].

### Preparation and structural studies

Compound **4** was isolated in reasonable yield from the reaction of ferrous chloride with two equivalents of the 2,3,4-trimethylpentadienyl anion ( $2,3,4\text{-C}_8\text{H}_{13}^-$ ). Like other reported methylated "open ferrocenes" [6,8], it is reasonably air-stable. The osmium derivative **3** was prepared in low yield (7.4%) by reduction of hydrated  $\text{Na}_2\text{OsCl}_6$  by zinc in ethanol solutions containing an excess of 2,4-dimethyl-1,3-pentadiene. The solid compound is essentially air-stable.

As various related "open ferrocenes" [6] and "open ruthenocenes" [5] have been found to exist in the unsymmetric *gauche*-eclipsed (I), rather than the *anti* (II), conformation, it was of interest to determine whether this would also hold for **3** and



**4**. In view of the finding that **5** prefers the *gauche*-eclipsed conformation even though it possesses two significant methyl-methyl non-bonded contacts, it was of interest to investigate the structural details of **3** and **4**. The latter compound should provide a particularly significant test of the *gauche*-eclipsed favorability, since in the *gauche*-eclipsed conformation the small iron atom will bring the two ligands into close proximity, thereby bringing about further destabilization of this conformation through methyl-methyl non-bonded repulsions. To check this possibility, variable temperature  $^1\text{H}$  NMR spectra of  $\text{Fe}(2,3,4\text{-C}_8\text{H}_{13})_2$  were recorded. At room temperature the expected four-line pattern was observed, but on cooling collapse of most of the resonances took place (with the exception of the central CH resonance), ultimately leading to a seven line pattern, indicative of an unsymmetric, presumably *gauche*-eclipsed, ground state.  $\Delta G^\ddagger$  for ligand oscillation was found to be  $9.4 \pm 0.1$  kcal/mol, slightly larger than that for **1** (9.1 kcal/mol) [9]. Furthermore an X-ray study on **4** has confirmed that the solid state structure is indeed *gauche*-eclipsed [10]. This seems to provide even stronger evidence for the stability of the *gauche*-eclipsed conformation.

In addition, variable temperature  $^1\text{H}$  NMR spectra for **3** clearly demonstrate that the complex contains an unsymmetric ground state, since at low temperature a seven line pattern of resonances is observed (vide infra). The barrier to ligand oscillation ( $\Delta G^\ddagger$ ) was found to be  $13.4 \pm 0.2$  kcal/mol [11], which compares with the smaller values of 9.1 and 9.7 kcal/mol observed for **1** and **4**, respectively.

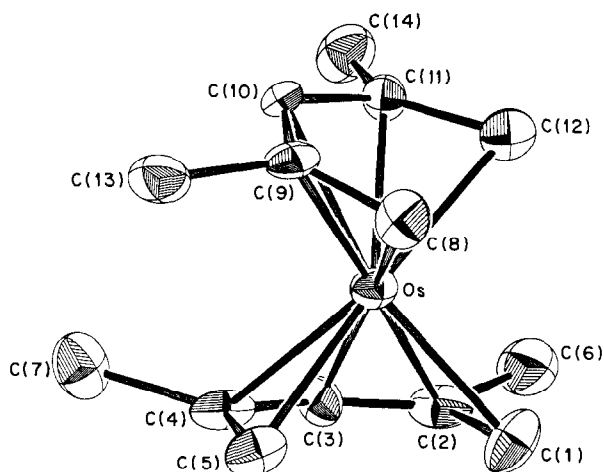


Fig. 1. Perspective view and numbering scheme for  $\text{Os}(\text{2,4-C}_7\text{H}_{11})_2$ .

An X-ray diffraction study confirmed the unsymmetric *gauche*-eclipsed conformation for **3** (see Fig. 1). Lists of atomic coordinates for non-hydrogen atoms are given in Table 1, and summarized in Tables 2 and 3. As in the case of the related iron and ruthenium analogs, the complex adopts the unsymmetric *gauche*-eclipsed conformation, in accord with the variable temperature NMR spectra. The experimental value of the conformation angle (relative to the *syn*-eclipsed conformation) is  $48.2^\circ$ , which compares with values of  $59.7^\circ$  for  $\text{Fe}(\text{2,4-C}_7\text{H}_{11})_2$  ( $\text{C}_7\text{H}_{11}$  = dimethylpentadienyl) and  $52.5^\circ$  for  $\text{Ru}(\text{2,3,4-C}_8\text{H}_{13})_2$ . It is not clear why the conformation angle departs from the ideal  $60^\circ$  value for the ruthenium and osmium complexes, although in approaching the *syn*-eclipsed conformation, the complex may be providing an open site to accommodate the lone pairs of electrons on the

TABLE 1

ATOMIC COORDINATES FOR THE NON-HYDROGEN ATOMS OF  $\text{Os}(\text{2,4-C}_7\text{H}_{11})_2$

Atom	x	y	z
Os	0.02832(10)	0.12963(6)	-0.19661(7)
C(1)	0.2141(28)	0.0291(17)	-0.0735(20)
C(2)	0.2040(27)	0.0107(15)	-0.2090(23)
C(3)	0.0636(26)	-0.0038(16)	-0.2917(22)
C(4)	-0.1011(37)	-0.0018(15)	-0.2990(18)
C(5)	-0.1345(31)	0.0057(15)	-0.1876(20)
C(6)	0.3627(27)	0.0263(19)	-0.2262(25)
C(7)	-0.2526(28)	0.0030(20)	-0.4211(21)
C(8)	-0.0486(25)	0.2330(18)	-0.0902(22)
C(9)	-0.1570(28)	0.2493(13)	-0.2071(20)
C(10)	-0.1027(28)	0.2627(15)	-0.3057(21)
C(11)	0.0718(25)	0.2545(16)	-0.2959(19)
C(12)	0.2014(26)	0.2528(16)	-0.1862(19)
C(13)	-0.3479(28)	0.2323(17)	-0.2491(23)
C(14)	0.1009(27)	0.2471(20)	-0.4148(22)

TABLE 2

PERTINENT BOND DISTANCES (Å) AND ANGLES (°) FOR Os(2,4-C<sub>7</sub>H<sub>11</sub>)<sub>2</sub>

Os-C(91)	2.20(2)	Os-C(8)	2.15(2)	C(1)-C(2)	1.63(3)	C(8)-C(9)	1.40(3)
Os-C(2)	2.23(2)	Os-C(9)	2.23(2)	C(2)-C(3)	1.27(3)	C(9)-C(10)	1.44(3)
Os-C(3)	2.20(2)	Os-C(10)	2.25(2)	C(3)-C(4)	1.39(4)	C(10)-C(11)	1.47(3)
Os-C(4)	2.20(2)	Os-C(11)	2.16(2)	C(4)-C(5)	1.48(3)	C(11)-C(12)	1.39(3)
Os-C(5)	2.19(2)	Os-C(12)	2.19(2)	C(2)-C(6)	1.47(3)	C(9)-C(13)	1.55(3)
				C(4)-C(7)	1.58(3)	C(11)-C(14)	1.55(3)
C(1)-C(2)-C(3)	120(3)	C(3)-C(4)-C(7)	123(3)	C(10)-C(9)-C(13)	112(2)		
C(1)-C(2)-C(6)	114(2)	C(5)-C(4)-C(7)	119(2)	C(10)-C(11)-C(12)	121(3)		
C(2)-C(3)-C(4)	135(4)	C(8)-C(9)-C(10)	124(3)	C(10)-C(11)-C(14)	116(2)		
C(3)-C(2)-C(6)	125(3)	C(8)-C(9)-C(13)	123(3)	C(12)-C(11)-C(14)	123(3)		
C(3)-C(4)-C(5)	118(2)	C(9)-C(10)-C(11)	124(3)				

metal atoms. While the qualitative structural features of the complex are quite clear, care must be taken in drawing quantitative comparisons. In part this is due to the presence of the heavy osmium atom, but in addition there is a problem with at least the C(2) center (see Table 2), whose bond distances appear quite suspect. Nonetheless, a few pertinent parameters merit discussion. The metal-bound portions of the pentadienyl ligands are planar within 0.07 Å, with the methyl groups tilted toward the osmium atom by an average of 11.1° (8.1, 13.4, 9.3, and 13.5°, respectively). Similar bendings of the 2- and 4-methyl groups have been observed for the iron and ruthenium analogs.

TABLE 3

DEVIATIONS (Å) OF ATOMS FROM BEST LEAST SQUARES PLANES

Atom	Dist.	Atom	Dist.
*C(1)	0.014	C(8)	2.799
*C(2)	-0.001	C(9)	3.222
*C(3)	-0.031	C(10)	3.544
*C(4)	0.045	C(11)	3.375
*C(5)	-0.027	C(12)	3.132
C(6)	0.207	C(13)	3.121
C(7)	0.365	C(14)	3.458
		Os	1.584
Equation: $-0.237x + 13.174y - 1.590z = 0.429$			
*C(8)	-0.029	C(1)	-2.735
*C(9)	0.013	C(2)	-3.185
*C(10)	0.037	C(3)	-3.496
*C(11)	-0.070	C(4)	-3.455
*C(12)	0.048	C(5)	-3.182
C(13)	-0.250	C(6)	-3.004
C(14)	-0.361	C(7)	-3.535
		Os	-1.571
Equation: $-0.093x + 13.222y + 1.492z = 2.988$			

The average Os–C bond distance is 2.200(7) Å, which compares with the values of 2.188(3) Å in Ru(2,3,4-C<sub>8</sub>H<sub>13</sub>)<sub>2</sub> [5], 2.196(3) Å in Ru(C<sub>5</sub>H<sub>5</sub>)<sub>2</sub> [12], and 2.178(3) and 2.168(3) Å for the C<sub>5</sub>H<sub>5</sub> and 2,4-C<sub>7</sub>H<sub>11</sub> ligands in Ru(C<sub>5</sub>H<sub>5</sub>)(2,4-C<sub>7</sub>H<sub>11</sub>) [13]. Despite the problems with C(2), all of the Os–C(*n*) bond distances (*n* = 1–5) are equivalent to those (*n* = 8–12) related by the molecular, non-crystallographic C<sub>2</sub> rotation axis. The average values for these pairs are 2.173(16), 2.228(13), 2.227(16), 2.182(15), and 2.190(5) Å, respectively. These lead to simplified values of 2.181(11), 2.205(10), and 2.227(16) Å for the generalized Os–C(1,5), Os–C(2,4) and Os–C(3) bond types. This pattern, while subject to substantial statistical uncertainty, most resembles that observed for V(2,4-C<sub>7</sub>H<sub>11</sub>)<sub>2</sub> [14], cf., 2.179(4), 2.231(4), and 2.236(5) Å, respectively.

A few comparisons may be made for the C–C bond distances and related angles. For the better-determined ligand defined by C(8)–C(14) there is the apparent usual shortening of the “external” vs. “internal” delocalized C–C bond distances (the respective averages being 1.395(22) and 1.453(23) Å) [5,6]. In addition, the presence of a methyl group on a given C–C–C bond angle also appears to bring about the usual contraction effect (Table 2) [5,6]. Finally, the C–CH<sub>3</sub> bond distances (excluding C(2)–C(61)) average 1.558(18) Å.

#### *Electronic structure of 1 and 1<sup>+</sup>*

The electronic structures of **1** and its congeners have already been discussed in detail [15,16] and therefore we only briefly summarize the results below. In Fig. 2 the

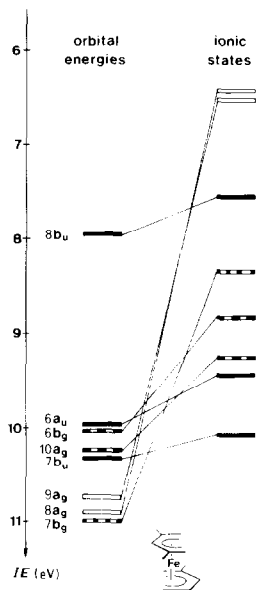


Fig. 2. Comparison between the calculated energies for **1** and the different ionic states calculated by using the Green's function technique. The full bars indicate orbitals which are localized at the ligands, empty bars stand for MOs which are localized at the metal. The numbering of the orbitals refers to the parent compound.

orbital sequences for **1** in its ground state (left) and its various ionic states (right) are compared. These results are based on an INDO calculation [17] for **1** in the *anti*-eclipsed conformation. The main reasons for using this conformation are first that the energy difference relative to the *gauche*-eclipsed form is relatively small (see above), second that the analyses of the wave functions are much easier with the higher symmetry, and third that comparison of the experimental ionization energies of **1** and its congeners with the calculated values derived by considering relaxation and correlation effects [15,16] reveals good agreement only if the *anti*-conformation is assumed.

To derive the energies of the ionic states we used the Green's Function formalism as discussed earlier [15]. The calculations reveal for the HOMO a pure ligand MO ( $8b_u$ ) [18] followed by two MOs whose wave functions are mixtures between  $3d$  orbitals of the Fe and ligand  $\pi$ -MOs ( $10a_g$ ,  $2b_g$ ). The next two MOs ( $6a_u$ ,  $2b_u$ ) are again localized on the ligands, followed by three MOs with heavy metal contributions.

As frequently observed the ionizations of transition metal compounds containing iron are characterized by Koopmans' defects which are proportional to the extent of localization at the metal center [16,17,19]. In the present case such localization occurs for  $9a_g$ ,  $8a_g$ , and to some extent for  $6b_g$ ,  $10a_g$ , and  $7b_g$  relative to the ligand MOs ( $8b_u$ ,  $6a_u$ ,  $7b_u$ ). As a result of these different Koopmans' defects the band sequence for **1**<sup>+</sup> is different from the sequence of the MOs in its ground state (see Fig. 2).

#### PE spectra of **1-6**

As representative of all six PE spectra, we show those of **1-3** in Fig. 3. The first ionization energies of **1-6** are listed in Table 4. A comparison of the PE spectra of **1** and **2** reveals considerable differences. While in **1** only four features are found below 10 eV, to which seven transitions can be assigned (see Fig. 2), six peaks are found in the case of **2**. Close inspection of the PE spectrum of **2** (Fig. 3) reveals three overlapping peaks of virtually the same intensity (bands 1-3) followed by a more intense one (band 4,5) well separated from the next two single bands (5 and 6). If we assign one ionization event to each of the latter two bands, we have to assign two ionization processes to the fourth (broad) peak. Figure 4 summarizes our comparison of the first PE band of **1** and **2**, and clearly reveals that the characteristic heavy atom effect is operative. The two close-lying transitions of the first and fourth peaks in the PE spectrum of **1** are clearly separated in that of **2** and **3**.

In our correlation between the first ionic states of **1** and **2** (Fig. 4), we assume that those bands which originate from metal orbitals (e.g.,  $9a_g$  and  $8a_g$ ) will be stabilized, while "ligand bands" remain constant or even be destabilized. This assumption is based on the comparison between the above-mentioned bis( $\eta^3$ -allyl) compounds of nickel, palladium, and platinum and between the  $\eta^3$ -allyl(tetra-carbonyl) [2] complexes of manganese and rhenium [3]. In all cases, the metal bands are shifted towards higher energy on going from the lighter to the heavier metal.

A comparison between the first PE bands of ferrocene with those of ruthenocene [20] furthermore confirms our correlation made in Fig. 4, in so far as the metal bands ( $3e_{2g}$ ,  $4a_{1g}$ ,  $3e_{1g}$ ) in the PE spectrum of ferrocene are shifted to higher energy in the PE spectrum of ruthenocene and the corresponding "ligand bands" ( $3e_{1u}$ ) shifted to lower energy. Comparison of the first three peaks of the PE spectrum of **1**

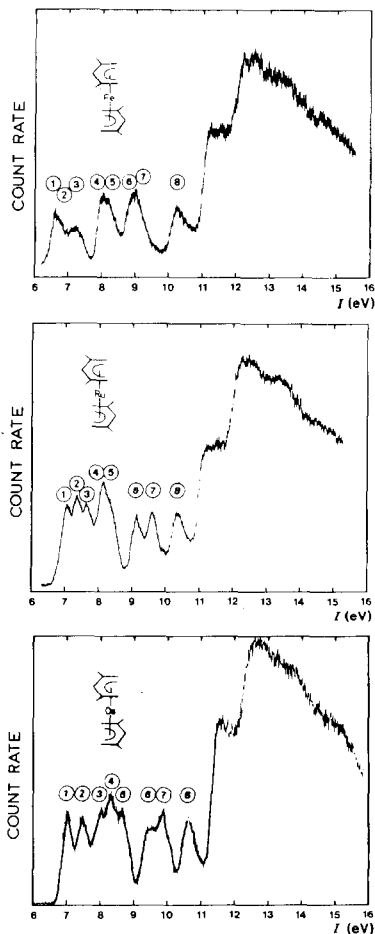


Fig. 3. He(I) PE spectra of 1–3.

with those for **3** (Fig. 4) shows clearly that the assignment of five different states to these peaks is reasonable.

Further confirmation of the assignments of the first five bands of **2** is found by

TABLE 4  
VERTICAL IONIZATION ENERGIES (eV) FOR 1–6

Compound	Band						
	1	2	3	4	5	6	7
<b>1</b>	6.63	6.7	7.2	8.0	8.13	8.9	9.2
<b>2</b>	7.05	7.45	7.6	8.1	8.25	9.1	9.6
<b>3</b>	7.05	7.45	8.05	8.3	8.65	9.5	9.9
<b>4</b>	6.4	6.5	7.0	8.26	8.36	9.6	9.8
<b>5</b>	6.9	7.3	7.6	7.9	8.1	9.05	9.4
<b>6</b>	6.2	6.7	6.8	7.1	7.3	8.1	8.7

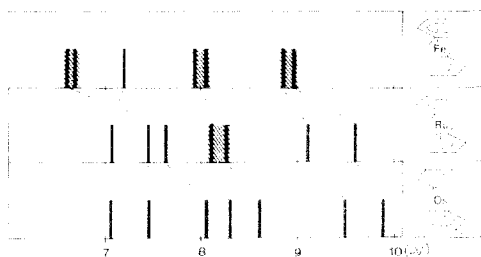


Fig. 4. Comparison of the first PE bands of **1-3**.

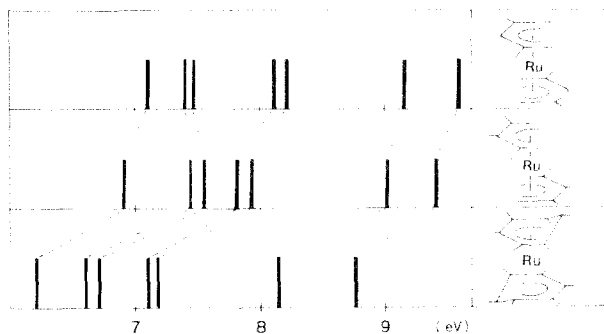


Fig. 5. Comparison between the first PE bands of **2, 5** and **6**.

considering the alkyl substituent effects between **2** and **5**. As mentioned previously, the MOs  $9a_g$  and  $8a_g$  are strongly localized at the metal while the metal character of the others varies between 0% ( $8b_u$ ,  $7b_u$ ) and 40% ( $10a_g$ ,  $7b_g$ ,  $6a_u$ ,  $6b_g$ ). From our previous experience with allyl complexes [2,3] we expected a shift towards lower energy for  $8b_u$  and  $7b_u$  as well as  $10a_g$ ,  $7b_g$ ,  $6a_u$ , and  $6b_g$  but no shift for  $9a_g$  or  $8a_g$ . As seen from Fig. 5, no shift is observed for bands 2 and 3 when the PE spectra of **2** are compared with those of **5**, but there is a shift towards lower energy for all the other bands between 0.1 and 0.3 eV.

## Conclusion

Our results suggest that as a result of replacing the lighter (iron) by heavier (ruthenium or osmium) metal there is a reversal of the first ionic state of **1** relative to that of **2** and **3**. For **1** the first ionic state is  ${}^2A_g$  while for **2** and **3**, it is  ${}^2B_u$ . This switch in the states (see Fig. 4) can be rationalized in terms of a smaller Koopmans' defect for  $9a_g$  and  $8a_g$  in the case of the heavier element. This can be explained by assuming a stronger overlap between ligands and metal in the case of the heavier metal atoms. This stronger overlap leads to a greater delocalization of  $9a_g$  and  $8a_g$ , and subsequently to smaller Koopmans' defects. As a corollary of this interpretation, we expect rather different ESR data for the radical cations of **1** and **4** relative to **2**, **3** and **5**. The observed higher  $\Delta G^\ddagger$  value for the ligand mobility of **4** compared with that of **3** is also in line with our proposal of increasing overlap with increasing nuclear charge.



## Experimental section

All operations involving organometallics were carried out under nitrogen in Schlenk apparatus or in a glovebox. Non-aqueous solvents were thoroughly dried and deoxygenated by standard methods and distilled immediately before use. Elemental analyses were performed by Micanal Laboratories. Anhydrous ferrous chloride was prepared as described by King [21].

### *Spectroscopic studies*

Infrared spectra were recorded with a Perkin–Elmer 298 spectrophotometer. Mulls were prepared in a glovebox with dry, degassed Nujol.  $^1\text{H}$  and  $^{13}\text{C}$  nuclear magnetic resonance spectra were recorded in toluene- $d_8$  on Varian EM-390, SC-300, and XL-300 spectrometers. Mass spectra (70 eV) were performed on a VG Micro-mass 7070 double focusing high resolution mass spectrometer with VG Data System 2000. Except for the parent fragment, peaks are only quoted if their relative intensities are at least 10% of the intensity of the strongest peak. Photoelectron spectra were recorded on a Perkin–Elmer PS18 photoelectron spectrometer with a He(I $\alpha$ ) lamp as the light source. The recording temperatures were: **1–5**, 70–80 °C and **6**, 120 °C. Calibrations were carried out with Ar and Xe. A resolution of about 20 meV on the argon line was obtained.

### *2,3,4-Trimethyl-1,3-pentadiene*

To 150 ml of a 1.50 *M* solution of methyllithium (225 mmol) in ether at –50 °C 13.0 g (91.6 mmol) of ethyl-2,3-dimethyl-2-butenolate [22] in 30 ml of ether was added dropwise with stirring during 2 h. The reaction solution was slowly warmed to room temperature and stirred overnight. It was then treated carefully with a slight excess of saturated aqueous  $\text{NH}_4\text{Cl}$ , then washed first with three 20 ml portions of water followed by three 20 ml portions of saturated aqueous NaCl. The ether layer was dried over magnesium sulfate and the ether removed in vacuo, 8.5 g (73%) of 2,3,4-trimethyl-3-penten-2-ol [23] was isolated by vacuum transfer. Complete infrared data (neat): 3380vs, vbr, 2975vs, 2920s, 2870sh, 1637m, 1465ms, sh, 1460ms, 1443ms, 1374s, 1360s, sh, 1312w, 1280w, 1260m, 1207m, 1194m, 1164s, 1138s, 1112s, 1090s, 1075ms, sh, 1048m, 946ms, sh, 940s, 890ms, 880m, sh, 837w, 801m  $\text{cm}^{-1}$ .  $^1\text{H}$  NMR:  $\delta$  2.28 (s, 1H), 1.98 (s, 3H), 1.70 (s, 6H), 1.41 (s, 6H).

On distillation of the alcohol from a small amount of iodine and glass wool, 2,3,4-trimethyl-1,3-pentadiene (b.p. 103–104 °C) was obtained in 65% yield. A similar dehydration of 2,3,4-trimethyl-4-penten-2-ol [24] also gave 2,3,4-trimethyl-1,3-pentadiene. In both cases the product was taken up in ether, the solution dried with  $\text{MgSO}_4$ , and pure product isolated by distillation. Complete infrared data (neat): 3070ms, 2965s, 2915vs, 2878s, 1630ms, 1460m, 1440s, 1370s, 1296w, 1133ms, 1110ms, 893vs  $\text{cm}^{-1}$ .  $^1\text{H}$  NMR:  $\delta$  4.88 (br, 1H), 4.62 (br, 1H), 1.75 (s, 3H), 1.69 (s, 9H).

### *(2,3,4-Trimethylpentadienyl)potassium, $K(2,3,4\text{-C}_8\text{H}_{13})$*

To 9.50 g (84.7 mmol) of  $\text{KOC}(\text{CH}_3)_3$  in 160 ml of hexane at 0 °C was added 8.50 g (77.1 mmol) of 2,3,4-trimethyl-1,3-pentadiene. Then 35 ml of a 2.50 *M* solution of butyllithium (87.5 mmol) in ether was added slowly from a syringe. After stirring of the reactants for 1.5 at room temperature, the yellow slurry was filtered off and dried in vacuo. Approximately 7.0 g (61%) of the crude salt was obtained.

*Bis(2,3,4-trimethylpentadienyl)iron, Fe(2,3,4-C<sub>8</sub>H<sub>13</sub>)<sub>2</sub>*

A slurry of 0.63 g (5.0 mmol) of ferrous chloride in 50 ml of THF was cooled with stirring to  $-78^{\circ}\text{C}$  under nitrogen, and a solution of 1.48 g (10.0 mmol) of the potassium salt of the 2,3,4-trimethylpentadienyl anion in 40 ml of THF was added dropwise. When the addition was complete, the mixture was slowly warmed to room temperature, after which time a deep red solution had been formed. The mixture was stirred overnight and the solvent then removed in vacuo and the product extracted with ca. 50 ml of pentane. The solution volume was reduced and some crude product was isolated by cooling to  $-78^{\circ}\text{C}$ , after which the supernatant solution was reduced in vacuo in volume to 5 ml, then cooled to  $-78^{\circ}\text{C}$  to yield a second batch of crystals. Most of the supernatant liquor was decanted and the rest removed by syringe, and the reddish crystalline product was dried first under a nitrogen stream and then in vacuo. Several recrystallizations were generally required to remove an unidentified brown impurity. The product was finally purified by sublimation at  $65^{\circ}\text{C}$  under high vacuum. Complete infrared data (Nujol mull): 3070m, 3050sh, 1260m, 1154m, 1103w, 1026s, 1016ms, 996s, 962w, 950w, 932ms, 913w, 840m, 779m, 730ms, 683ms  $\text{cm}^{-1}$ .  $^1\text{H}$  NMR:  $\delta$  2.54 (d, 2H,  $J$  2 Hz), 1.61 (s, 6H), 1.52 (s, 3H), 0.18 (d, 2H,  $J$  2 Hz).  $^{13}\text{C}$  NMR:  $\delta$  100.4 (s, 1C), 95.0 (s, 2C), 52.6 (t, 2C,  $J$  155.8 Hz), 24.6 (q, 2C,  $J$  126.5 Hz), 15.2 (q, 1C,  $J$  126.5 Hz). Mass spectrum:  $m/e$  (relative intensity): 39(11), 41(20), 56(41), 67(11), 71(11), 91(11), 96(32), 108(14), 110(27), 124(36), 148(16), 162(34), 164(100), 165(12), 167(27), 274(52), 275(11). Anal. Found: C, 70.08; H, 9.72.  $\text{C}_{16}\text{H}_{26}\text{Fe}$  calc: C, 70.06; H, 9.57%.

*Bis(2,4-dimethylpentadienyl)osmium, Os(2,4-C<sub>7</sub>H<sub>11</sub>)<sub>2</sub>*

Absolute ethanol (14 ml) was freeze-thaw degassed in a 100-ml 3-neck flask equipped with nitrogen inlet and magnetic stirring bar. A sample of 1.00 g (2.18 mmol) of  $\text{Na}_2\text{OsCl}_6 \cdot x\text{H}_2\text{O}$  (Alfa, 41.37% Os) was dissolved in the ethanol, to give a green-brown solution. Approximately 5.0 ml (42 mmol) of previously degassed 2,4-dimethyl-1,3-pentadiene was then added from a syringe, followed by 3.2 g (49 mmol) of zinc powder (Fisher). The solution was refluxed under nitrogen for about 24 h, during which its color gradually changed from green-brown to very dark brown. The mixture was then allowed to cool and the ethanol and excess diene were removed in vacuo to leave a dark brown granular solid. This residue was exhaustively extracted with 300 ml of pentane and the light yellow solution filtered through a Celite pad on a coarse frit then concentrated to 10 ml. After 4 d at  $-98^{\circ}\text{C}$ , 61 mg (0.16 mmol) of pale yellow (almost colorless) crystals (m.p.  $101\text{--}102^{\circ}\text{C}$ ) were isolated. The yield was 7.4% based on  $\text{Na}_2\text{OsCl}_6 \cdot x\text{H}_2\text{O}$ . Anal. Found: C, 44.21; H, 5.69.  $\text{C}_{14}\text{H}_{22}\text{Os}$  calc: C, 44.19; H, 5.83%. Complete infrared data (Nujol mull): 3050m, 3034s, 3026ms, 3012ms, 1480sh, 1442vs, 1427vs, 1342m, 1276ms, 1058w, 1027vs, 1013m, 988ms, 967s, 937m, 920m, 912m, 850vs, 832w, 821w, 779ms, 723mw.  $\text{cm}^{-1}$ .  $^1\text{H}$  NMR (toluene- $d_8$ ,  $-28.6^{\circ}\text{C}$ ):  $\delta$  5.03 (s, 2H), 3.99 (d, 2H,  $J$  3.4 Hz), 2.22 (d, 2H,  $J$  1.7 Hz), 1.72 (s, 6H), 1.70 (s, 6H), 1.67 (d, 2H,  $J$  3.2 Hz), 0.40 (s, 2H).  $^1\text{H}$  NMR (toluene- $d_8$ ,  $94.0^{\circ}\text{C}$ ):  $\delta$  5.23 (s, 2H), 3.01 (s, 4H), 1.79 (s, 12H), 0.94 (s, 4H).  $^{13}\text{C}$  NMR (toluene- $d_8$ ,  $99.1^{\circ}\text{C}$ ):  $\delta$  100.7 (d,  $J$  157 Hz), 91.0 (s), 35.8 (t,  $J$  154 Hz), 26.1 (q,  $J$  128 Hz). Mass spectrum (EI, 70 eV):  $m/e$  (relative intensity): 186(10), 188(16), 189(12), 254(14), 254(12), 255(13), 266(10), 278(13), 280(15), 293(11), 306(13).

307(14), 320(12), 321(12), 322(14), 324(19), 334(13), 336(14), 338(16), 349(13), 360(52), 362(23), 363(75), 364(20), 365(24), 376(100), 379(47), 380(61), 381(11), 382(54).

*X-ray diffraction study of Os(2,4-C<sub>7</sub>H<sub>11</sub>)<sub>2</sub>*

Attempts to grow single crystals of this compound by slow cooling of concentrated hydrocarbon solutions did not work well. Better crystals were obtained by slow sublimation, but even these formed as clusters. However, some of the latter were carefully cut to yield apparent singly crystalline fragments. One such fragment, of approximate dimensions 0.15 × 0.20 × 0.30 mm, was used for the single crystal study. Oscillation and Weissenberg photography indicated a monoclinic unit cell, and subsequent examination of the systematic absences revealed the space group to be  $C_{2h}^2-P2_1/n$  (No. 14). After the crystal was transferred to a Stoe-Siemens diffractometer, the unit cell parameters were determined from 30 centered reflections, leading to the values  $a = 8.590(7)$ ,  $b = 13.333(9)$ ,  $c = 12.098(5)$  Å,  $\beta = 111.24(5)^\circ$ ,  $V = 1291.5$  Å<sup>3</sup> for  $Z = 4$ , using Mo- $K_\alpha$  radiation ( $\lambda = 0.71069$  Å).

Data collection was carried out in the  $\theta-2\theta$  mode, with  $3^\circ < 2\theta < 60^\circ$ . Using a variable scan rate of 2.5–29.5° min<sup>-1</sup>, a total of 2577 reflections were measured, of which 2418 were considered observed ( $I > 2.5\sigma(I)$ ). The intensities of two reflections were measured for every 100 reflections, and displayed no variation. Calculations were carried out with the SHELXTL Version 5.1 programs, and an empirical absorption correction was applied using  $\psi$ -scan data for six reflections in the range of  $4.7^\circ < 2\theta < 39.9^\circ$ . The relative range in transmission factors was found to be 0.5226–1.0000, which may be compared to the calculated linear absorption coefficient of 94.46 cm<sup>-1</sup>.

The position of the osmium atom was readily determined from a Patterson map, and all remaining non-hydrogen atoms were subsequently located on a difference Fourier map. Following subsequent anisotropic refinement, hydrogen atoms were placed in calculated positions with  $d(C-H)$  0.96 Å, and isotropic thermal parameters roughly equal to the equivalent isotropic thermal parameters for the carbon atoms to which they were attached. Final refinement led to agreement indices of  $R = 0.075$  and  $R_w = 0.066$ . The largest peak in the final difference Fourier map was near the osmium atom, with a height of 3.04 e/Å<sup>3</sup>. No unusual intermolecular contacts were observed. Lists of atomic coordinates for non-hydrogen atoms are given in Tables 1 and 2 and detail of relevant bonding parameters in Tables 3 and 4. Tables of anisotropic thermal parameters, hydrogen atom coordinates and structure factors have been submitted to NAPS.

### Acknowledgement

R.D.E. expresses his gratitude for support of this research from the National Science Foundation, and from the donors of the Petroleum Research Fund of the American Chemical Society. R.G. and M.L.Z. thank the Deutsche Forschungsgemeinschaft for their support. R.D.E. and R.G. are also grateful to NATO for a travel grant which made this work possible. We thank Prof. Virgil Boekelheide for kindly providing the sample of **6**.

## References

- 1 M.C. Böhm and R. Gleiter, *Angew. Chem.*, 95 (1983) 334; *Angew. Chem. Int. Ed. Engl.*, 22 (1983) 329.
- 2 M.C. Böhm, R. Gleiter, and R. Batich, *Helv. Chim. Acta.* 63 (1980) 990.
- 3 M.C. Böhm, R. Gleiter, T.A. Albright, and V. Sriyonyongwat, *Mol. Phys.*, 50 (1983) 113.
- 4 D.R. Wilson, A.A. DiLullo, and R.D. Ernst, *J. Am. Chem. Soc.*, 102 (1980) 5928.
- 5 L. Stahl and R.D. Ernst, *Organometallics*, 2 (1983) 1229.
- 6 R.D. Ernst, *Acc. Chem. Res.*, 18 (1985) 56.
- 7 R.T. Swann, A.W. Hanson, and V. Bockelheide, *J. Am. Chem. Soc.*, 108 (1986) 3324.
- 8 D.R. Wilson, R.D. Ernst, and T.H. Cymbaluk, *Organometallics*, 2 (1983) 1220.
- 9 It should be noted that in the other "open ferrocene" compounds, as well as the "open ruthenocenes", the addition of a methyl group resulted in an increase in  $\Delta G^\ddagger$  by ca. 0.4 kcal/mol.
- 10 J.-C. Han, J.P. Hutchinson and R.D. Ernst, *J. Organomet. Chem.*, 321 (1987) 389.
- 11 H. Kessler, *Angew. Chem. Int. Ed. Engl.*, 9 (1970) 219.
- 12 (a) A. Haaland and J.E. Nilsson, *Acta. Chem. Scand.*, 22 (1968) 2653; (b) G.L. Hardgrove and D.H. Templeton, *Acta Crystallogr.*, 12 (1959) 28.
- 13 G. Sergeson and M.L. Ziegler, unpublished results.
- 14 C.F. Campana, R.D. Ernst, D.R. Wilson, and J.-Z. Liu, *Inorg. Chem.*, 23 (1984) 2732.
- 15 M.C. Böhm, M. Eckert-Maksic, R.D. Ernst, D.R. Wilson, and R. Gleiter, *J. Am. Chem. Soc.*, 104 (1982) 2699.
- 16 R. Gleiter, M.C. Böhm, and R.D. Ernst, *J. Electron Spectrosc. Rel. Phen.*, 33 (1984) 269.
- 17 M.C. Böhm and R. Gleiter, *Theor. Chim. Acta.* 57 (1980) 315.
- 18 We assume the same numbering scheme as in the parent compound.
- 19 M.C. Böhm and R. Gleiter, *J. Comput. Chem.*, 3 (1982) 140; M.C. Böhm, *Theor. Chim. Acta.* 61 (1982) 539; *Int. J. Quant. Chem.*, 22 (1982) 939.
- 20 S. Evans, M.L.H. Green, B. Terohi, A.F. Orchard, and C.F. Pygall, *J. Chem. Soc., Faraday Trans. II*, 68 (1972) 1874.
- 21 R.B. King, *Organometallic Syntheses*, Academic Press, New York, I (1965) 73.
- 22 K. Okada, F. Kiyooka, E. Nakanishi, M. Hirano, I. Ohno, N. Matsuo, and M. Matsui, *Agric. Biol. Chem.*, 44 (1980) 2595.
- 23 M.B. Green and W.J. Hickinbottom, *J. Chem. Soc.*, (1957) 3262.
- 24 (a) F. Sato, H. Ishikawa, and M. Sato, *Tetrahedron Lett.* (1980) 365; (b) N.C. Deno, H.G. Richey, Jr., N. Friedman, J.D. Hodge, J.J. Houser, and C.U. Pittman, Jr., *J. Am. Chem. Soc.*, 85 (1963) 2991.